MECOM permits pancreatic acinar cell dedifferentiation avoiding cell death under stress conditions

Running title: MECOM permits acinar cell dedifferentiation

Backx Elyne [1], Wauters Elke [2], Baldan Jonathan[2], Van Bulck Mathias[1], Michiels Ellis[1], Heremans Yves[1,3], De Paep Dieter Luc [4], Bouwens Luc [2], Kurokawa Mineo [5], Goyama Susumu [5], Jacquemin Patrick [6], Houbracken Isabelle[1,2], Rooman Ilse[1]

[1] Laboratory of Medical and Molecular Oncology, Oncology Research Centre, Vrije Universiteit Brussel, Brussels, Belgium

[2] Cell Differentiation Laboratory, Vrije Universiteit Brussel, Brussels, Belgium

[3] Laboratory of Beta Cell Neogenesis, Vrije Universiteit Brussel, Brussels, Belgium

[4] Beta Cell Bank, Diabetes Research Center, UZ Brussel, Brussels, Belgium

[5] Department of Hematology and Oncology, Graduate School of Medicine, The University of Tokyo, Tokyo, Japan

[6] Laboratory of Liver and Pancreatic Differentiation, De Duve Institute, Université Catholique de Louvain, Brussels, Belgium

Corresponding author: Ilse Rooman, irooman@vub.be

ABSTRACT

Maintenance of the pancreatic acinar cell phenotype suppresses tumor formation. Hence, repetitive acute or chronic pancreatitis, stress conditions in which the acinar cells dedifferentiate, predispose for cancer formation in the pancreas. Dedifferentiated acinar cells acquire a large panel of duct cell specific markers. However, it remains unclear to what extent dedifferentiated acini differ from native duct cells and which genes are uniquely regulating acinar cell dedifferentiation. Moreover, most studies have been performed in mouse since the availability of human cells is scarce.

Here, we applied a non-genetic lineage tracing method in our culture model of human pancreatic exocrine cells that allowed cell-type specific gene expression profiling by RNA sequencing. Subsequent to this discovery analysis, one transcription factor that was unique for dedifferentiated acinar cells was functionally characterized using *in vitro* and *in vivo* genetic loss-of-function experimental models.

RNA sequencing analysis showed that human dedifferentiated acinar cells expressed genes in 'Pathways of cancer' with prominence of the transcription factor *MECOM (EVI-1)* that was absent from duct cells. During mouse embryonic development, pre-acinar cells transiently expressed MECOM and MECOM was re-expressed in experimental *in vivo* models of acute and chronic pancreatitis *in vivo,* conditions in which acinar cells dedifferentiate. MECOM expression correlated with and was directly regulated by SOX9. MECOM loss-of-function in mouse acinar cells *in vitro* and *in vivo* impaired cell adhesion resulting in more prominent acinar cell death and suppressed acinar cell dedifferentiation by limiting ERK signaling.

In conclusion, we transcriptionally profiled the two major human pancreatic exocrine cell types, acinar and duct cells, during experimental stress conditions. We provide insights that in dedifferentiated acinar cells, cancer pathways are upregulated in which

MECOM is a critical regulator that suppresses acinar cell death by permitting cellular dedifferentiation.

INTRODUCTION

Few cancers have such poor survival rates as pancreatic ductal adenocarcinoma (PDAC) (1). Understanding the molecular mechanisms that are at play in early stage cancer formation is important to improve disease outcomes, but clinical samples of early disease are rare. Hence, genetically modified mouse models are pivotal to provide us insight into the contribution of the different pancreatic cell types to tumor formation (2-4). Accumulating evidence points to acinar cells as cells of origin for pancreatic tumor development (5-10). In order to become susceptible to tumorigenesis, acinar cells have to lose their differentiated phenotype to some extent. Consequently, tumorigenesis. is restrained by mechanisms that control acinar cell differentiation (5-10). Loss of differentiation can result from repetitive acute or chronic pancreatitis whereby dedifferentiated acinar cells acquire a panel of markers that are typical for (embryonic) duct cells (11-13). Notably, duct cells can also give rise to tumors but likely through on other mechanisms (14-16).

To date, knowledge is lacking to discriminate the mechanisms that govern the duct-like dedifferentiated acinar cell phenotype versus the 'native' duct cell phenotype, the latter being more resistant to stress- or inflammation-associated tumorigenesis. Previously, we had established *in vitro* experimental models that recapitulate a human (12) and rodent (13) acinar dedifferentiation. Specifically, upon suspension culture acinar cells lose their acinar-specific markers while gaining (embryonic) duct-like features, thereby mimicking chronic pancreatitis(12, 13).Here, we investigated the differential gene expression in adult human dedifferentiated acinar cells compared to

native duct cells from the same cell preparations. The transcription factor *MECOM/EVI-1* was found to be uniquely re-expressed in dedifferentiated acinar cells since embryonic development.

Although *MECOM* transcription factor is a known oncogene with a role in apoptosis (17-19) and pancreatic tumor formation (20, 21), its function in acinar cell (de)differentiation is still unknown. We analyzed its role in the context of acinar cell dedifferentiation through caerulein-induced pancreatitis modeling in transgenic *Evi-1* knock-out mice. We provide mechanistic insights that mouse acinar cells are dependent on MECOM expression to prevent cell death by allowing them acquisition of the dedifferentiated cell state.

MATERIALS AND METHODS

Human donor material and cell culture

Human pancreata from deceased donors were processed by the Beta Cell Bank of the Centre for Beta Cell Therapy in Diabetes (Brussels, Belgium), affiliated to the Eurotransplant Foundation (Leiden, The Netherlands). Consent for the use of residual donor material for research was obtained according to the legislation in country of organ procurement. This project was approved by the Medical Ethical Committee of UZ Brussel - Vrije Universiteit Brussel (B.U.N. 143201732260). Human exocrine cells were cultured as previously described (11, 12).

Mouse strains and experiments

ElaCreERT mice (22) ElaCreERT;Sox9$^{f/f}$ (23) (kindly provided by P. Jacquemin (UCL, Belgium) originally from D. Stoffers (UPenn, USA)) were crossed with EVI-1exon4 loxP mice (*Mecom*$^{f/f}$) (24) (kindly provided by M. Kurokawa, UPenn), resulting in

ElaCreERT;*Mecom*$^{f/f}$ mice (Mecom KO). ElaCreERT;*Sox9*$^{f/f}$ (23) were kindly provided by P. Jacquemin (UCL, Belgium). Six to eight-weeks-old ElaCreERT;*Mecom*$^{f/f}$ and ElaCreERT;Sox9$^{f/f}$ mice received tamoxifen and (Z)-4-Hydroxytamoxifen (all from Sigma-Aldrich, St-Louis, MO, USA) and were treated with 1,25mg/kg body weight caerulein (Invitrogen Waltham, Massachusetts, USA) according to (23). Acinar cell isolation was adapted from (13). Embryonic mouse tissue was isolated from ElaCreERT mice at E16.5 timepoint of embryonic development. All animal experiments were approved by the Ethical Committee for Animal Testing at the Vrije Universiteit Brussel (#17-637-1).

Fluorescent activated cell sorting (FACS)

FITC-conjugated UEA-1 (*Ulex Europaeus* Agglutinin-1, Sigma-Aldrich) lectin labeling of acinar cells within the human exocrine cell fraction was performed as in (12). At day 4 of suspension culture, cell clusters were dissociated following the protocol of (11). Analysis and cell sorting were performed on a BD FACSAria (BD Biosciences, Franklin Lakes, NJ, USA). Viable, single cells were gated based on forward and side scatter.

More details on experimental design and statistics can be found in supplementary materials and methods.

Results

MECOM is a cancer-related transcription factor uniquely expressed in human dedifferentiated acinar cells

Given the difference in propensity of dedifferentiated acinar cells and duct cells for pancreatitis-associated tumor development (5), we were specifically interested in the

differential gene expression of these two populations. Using the acinar-specific UEA-1 lectin in combination with the duct cell marker CA19.9, we FACS-purified both cell populations (11, 12) (Figure 1a,b). We confirmed the mutually exclusive expression pattern of CD142, a progenitor marker (11) in the UEA1+ dedifferentiated acinar cells, and of CA19.9 in the UEA1- duct cells (Figure 1b). We validated the different expression levels of the acinar cell markers MIST-1 and chymotrypsin, the progenitor marker CD142 and the duct-cell marker CK19 in the original mixed exocrine cell fraction and in the purified dedifferentiated acinar cells (UEA1+/CA19.9-) and native duct cells (UEA1-/CA19.9+) (Supplementary Figure 1). Comparing dedifferentiated acinar cells with native duct cells by RNAseq analysis highlighted 7953 differentially expressed genes (Adj. p<0,01). Of these, 1219 genes were expressed higher in dedifferentiated acinar cells (log fold change (FC) of ≤-2; Adj. p<0,01) (Supplementary Table 1) and were enriched for the KEGG pathways (Adj. p<0.01): 'Protein digestion and absorption' and 'Pancreatic secretion', including genes such as carboxypeptidase A and amylase, pointing to gene expression reminiscent of the abundant acinar cell transcriptome (25). In addition, 'Pathways in cancer' belonged to the top enriched pathways such as those of the WNT signaling pathway, which is well-known for its function in pancreatic tumorigenesis. Other enriched pathways included 'PI3K-AKT signaling', which is involved in acinar cell dedifferentiation and pancreatic tumorigenesis (26-28) and 'Complement and coagulation cascades' encompassing genes belonging to the tissue damage pathway (Figure 1c) and that code for F8, fibrinogen and F3 (CD142), the marker used above (11) (Figure 1b).

Dedifferentiated acinar and duct cells did have equal expression of the embryonic precursor gene *PDX1*, confirming our previous work (13). *PTF1A*, *NR5A2*, *RBPJL*, *FOXA3* and *GATA4* were expressed higher in the dedifferentiated acini reminiscent of

their fully differentiated state. Of note, *GATA6* expression, which is required for embryonic acinar cell differentiation (29, 30) and a suppressor of pancreatic carcinogenesis (31, 32), was not different from the duct cells.

Conversely, duct cell-enriched genes included *CFTR*, *SOX9*, *NKX6.1*, *HES1*, *HNF1B* and *ONECUT2* (*HNF6B*), established markers of duct cell differentiation. The most significantly duct cell-enriched gene was *DCDC2* (Doublecortin Domain Containing 2), demonstrated to bind tubulin and enhance microtubule polymerization (33) (Figure 1d). In the duct cell fraction, we found KEGG pathway enrichment for 'ECM receptor pathway interaction' and 'O-linked glycosylation'. Also, here, 'Pathways in cancer' featured here but the genes in this pathway differed from the ones in the dedifferentiated acinar cell fraction (Supplementary Table 1).

Among the differentially expressed genes were 71 transcription factors. The most significantly enriched transcription factor in the dedifferentiated acinar cell fraction was *MECOM* (log2FC = -6,09; Adj. p = 1,04E-123) (Figure 1d, Supplementary Table 1). *MECOM*, a known oncogene (34-36). It has been described as an activator of KRAS and glypican-1 in pancreatic cancer (20, 21). During our study, it was reported in relation to acinar cell-derived tumorigenesis (37). Hence, we confirmed *MECOM* expression in human PDAC samples (N=3) (Supplementary Figure 2a). We also used RNAseq analysis of stage 1 and 2 PDAC (N=103) where it correlated positively with overall survival (Supplementary figure 2b). In the same cohort, we previously reported a similar pattern for *SOX9* and a correlation in expression between *SOX9* and *MECOM* (Pearson R=0,49) (23). Pathway analysis of genes correlating with MECOM (Supplementary figure 2c) revealed similar pathways as those reported in our study on SOX9 where regulation of ErbB signaling was highlighted (23).

In conclusion, we FACS-purified human dedifferentiated acinar and duct cells and analyzed their transcriptome. The dedifferentiated acinar cell fraction showed a signature reminiscent of the acinar cell identity and specifically expressed *MECOM*, a transcription factor that featured in the pathway 'Pathways of cancer'. MECOM was expressed in PDAC where it correlated with SOX9. We hypothesized that MECOM plays a role during acinar cell dedifferentiation, an event that initiates pancreatic tumor development.

MECOM is expressed in developing acinar cells and is re-expressed during pancreatitis-associated acinar cell dedifferentiation

We comprehensively assessed expression of MECOM during acinar cell differentiation or loss thereof.

First, we confirmed the differential expression of *MECOM* in the purified human dedifferentiated acinar and duct cells from the experiments above (Figure 2a). Using RISH, *MECOM* mRNA appeared expressed at low levels in the acinar compartment of normal human pancreas (0,24±0,09 mRNA dots/cell; N=3), but increased strongly in samples of chronic pancreatitis (1,46±0,10 mRNA dots/cell; N=3) (Figure 2b,c).

Within the human purified dedifferentiated acinar cell fraction, *MECOM* showed strong correlation with *CD142* (Pearson R = 0,926, adj. P < 0,01), as discussed before (Figure 1). Immunofluorescent co-staining of MECOM and CD142 after 4 days of culture showed strong colocalization of the two proteins (56,94±10,63% MECOM+/CD142+ cells; N=5), while MECOM did not co-localize with the duct cell marker CK19 (5,69±2,32% MECOM+/CK19+ cells; N=5) (Figure 2d,e).

Next, we assessed the expression pattern (Figure 2f-i) and levels (Figure 2j) of *Mecom* mRNA in murine pancreas. In contrast to normal adult mouse pancreas where *Mecom*

was expressed at very low levels (Figure 2f,j) a significantly increased expressed was noted in E16.5 pancreas where it localized to pro-acinar tip cells (Figure 2g,j) (38, 39). Similar to human, *Mecom* became re-expressed during acute and chronic pancreatitis in mouse (Figure 2h,i,j).

Altogether, these data show that *Mecom* is transiently expressed in developing acinar cells and becomes re-expressed during pancreatitis in dedifferentiated acinar cells.

SOX9 regulates *Mecom* expression in dedifferentiated acinar cells

SOX9 is an important marker of acinar cell dedifferentiation and is indispensable for tumor formation in the pancreas (23). SOX9 correlates with MECOM in PDAC patients, as shown above, but also in other tissues (40, 41). Hence, we investigated whether these two transcription factors might also correlate in the context of acinar cell dedifferentiation. Indeed, we observed a strong correlation between *MECOM* and *SOX9* (Pearson R = 0,83; *p=0,015; N=6) (Figure 3a) in the human exocrine cell cultures in which acinar cells gradually dedifferentiate, a finding which was confirmed at the protein level (Figure 3b).

Based on the observed induction of *Mecom* after 48 hours of caerulein-induced acute pancreatitis (Figure 2h), we investigated *Mecom* expression in *Sox9* loss-of-function mice (Figure 3c) (13, 42). ElaCreERT;*Sox9*$^{f/f}$ mice showed significant reduction in *Mecom* compared to control mice (ElaCreERT) (19,48 ± 4,54% reduction in mRNA dots) (Figure 3c). suggestive for SOX9 to act as an upstream regulator of *Mecom*.

To further study whether SOX9 directly regulated *Mecom* in the acinar cell context, we performed a promoter-reporter assay on the partially differentiated mouse acinar cell line 266-6 (that expresses *Mecom*, as shown further). We observed low increase in luciferase activity when cells were transfected with the *Mecom* enhancer expression

plasmid alone. After *Sox9* overexpression, luciferase activity increased significantly (Figure 3d), indicating that SOX9 regulates the Mecom enhancer in partially differentiated acinar cells.

In conclusion, we showed that *Mecom* is (directly) regulated by SOX9 in pancreatic acinar cell context.

Mecom maintains cell adhesion and cell viability in a partially differentiated acinar cell line and in human and mouse acinar cell cultures

A lentiviral all-in-one CRISPR/Cas9-mediated approach comparing 3 different gRNAs designed to knock out (KO) *Mecom* in a partially differentiated acinar cell line (266-6) (Supplementary Figure 3), enabled us to study the role of Mecom in acinar cell dedifferentiation. RISH for *Mecom* in the loss-of-function condition (Figure 4a) showed significant reduction of mRNA expression (27,30±4,25% dots/cell decrease). In the Mecom KO condition, the cells were not able to organize into the typical 'acinar dome-like' structures that were observed in the cells transduced with non-targeting gRNA (Figure 4b), suggestive of loss of proper cell-cell contacts. We also observed a decrease in absolute cell number (Figure 4c), an overall diminished cell viability (Figure 4d) and a significant increase in cleaved caspase 3+ cells (Figure 4e), all indicative of cell death.

We further studied downstream transcriptional effects of Mecom loss in this cell line by RNAseq analysis. Differential gene expression analysis revealed downregulation of genes enriched in 'Focal adhesion', 'ECM receptor interaction' and 'Pathways in cancer' (Figure 4f). This supported our observations of diminished dome formation due to potentially impaired cell adhesion. We also compared the differentially expressed genes from the Mecom KO condition with a publicly available MECOM ChIP-Seq

dataset (43) and found several overlapping genes (Figure 4g) that we further considered, in particular integrins that link the extracellular matrix (ECM) components such as collagen to the cytoskeleton. The data suggested that loss of *Mecom* might compromise cell-cell interaction by diminished Collagen IV-Integrin a2 interaction and downstream ERK-mediated signaling (Figure 4h), the latter considered crucial in acinar cell dedifferentiation (44).

Diminished expression of collagen type IV and reduced ERK signaling upon Mecom loss-of-function was confirmed by immunofluorescent staining (Figure 4i,j).

In conclusion, *Mecom* is indispensable to maintain cell adhesion and cell viability in a partially differentiated acinar cell line.

Next, we crossed ElaCreERT deletor mice with mice carrying a floxed exon 4 of *Evi*, an exon which is conserved in all transcript variants (24) (Figure 5a). We studied effects in dedifferentiated acinar cells isolated from these mice using an established cell culture model, similar to the human cell culture model described above (13). Immunohistochemical staining for MECOM showed 42,71±13,42% less MECOM positive cells in freshly isolated (day 0) MECOM KO exocrine cells, consistent with previous reports on the recombination efficiency of the ElaCreERT strain (45-47). Interestingly, by day 4, we detected only 23,89±13,42% less MECOM positive cells in the KO condition suggesting selective loss of MECOM deficient cells (Supplementary Figure 4).

We observed that after cell isolation the control cells remained organized in small acinar spheroid-like structures while in the MECOM KO condition they often presented as single cells. After 4 days of culture, clusters did form in the ElaCreERT;*Mecom*$^{f/f}$ mouse cells but cluster diameter was significantly smaller compared to those of ElaCreERT control mice (57,21±15,73% reduction in average diameter) (Figure 5b,e),

suggestive of diminished cell adhesion and cell death of the single cells. In our experience acinar cells cannot survive as single cells (e.g. after FACS purification).

Similar to our results in the 266-6 cells (Figure 4), an increased fraction of acinar cells in the MECOM KO cultures stained positive for cleaved caspase 3 (81,21±26,47% increase in cleaved caspase 3+ cells) (Figure 5c,f). Notably, the MECOM KO cultures also showed fewer expression of CK19+ cells in comparison to the control cells (25,79±6,33% reduction in CK19+ cells), suggesting a lower capacity for dedifferentiation (Figure 5d,g).

These observations were confirmed by shRNA-mediated knockdown in cultured human exocrine cells in culture. At 24h, 4 and 7 days after transduction, average cluster diameter was significantly decreased (Supplementary Figure 5), underscoring the compromised cell-cell adhesion.

In conclusion, MECOM is indispensable for maintenance of cell-cell adhesion and cell viability in primary cultures of mouse and human acinar cells.

Mice with *Mecom*-deficient acinar cells show impaired recovery from acute pancreatitis

Since the primary cell culture models above recapitulate acinar cell dedifferentiation as it occurs during pancreatitis (11-13), we subjected control and MECOM KO mice to caerulein-induced acute pancreatitis. In wild-type mice, acute pancreatitis peaks around day 4 and resolves by day 11 (Figure 6a). We observed no macroscopic differences in the pancreas nor in weight of the pancreas or body weight when comparing Mecom-deficient with control mice (Supplementary Figure 6). Haematoxylin-eosin staining however showed more inter-acinar spaces at day 11 in the Mecom KO mice (Figure 6b,f). Similar to the phenotype observed in the 266-6 cells

(Figure 4) and the *ex vivo* cultures (Figure 5), this was preceded by an increased incidence of apoptosis (Figure 6c,g). Since we observed more inter-acinar space in the Mecom KO mice, we analyzed immune cell infiltration. Similar to a previous report (37), at day 11, CD3 positive area in MECOM KO mice remained at a level comparable to the acute phase of pancreatitis (day 4) whereas in the control mice it was significantly decreased (Figure 6e,i). F4/80+ macrophages showed a similar trend (not shown). Remarkably, no difference in collagen deposition could be detected between control and MECOM KO mice (Figure 6d,h) indicating that the inter-acinar space was not filled with collagen. The histological pattern showing accumulation of excessive liquid in the interstitial space was consistent with that of edema. Also, we did not observe any changes in acinar-to-ductal transdifferentiation markers at day 11 (not shown).

Altogether, these results indicate that MECOM-deficiency in pancreatic acinar cells under the experimental stress of acute pancreatitis leads to increased acinar cell death with ensuing immune cell infiltration and edema.

Discussion

When subjected to stress, such as occurring during chronic pancreatitis, acinar cells dedifferentiate and acquire a ductal cell-like phenotype, rendering them prone to *Kras* induced transformation, in contrast to the native duct cells which seem more resistant to neoplastic development. Where studies in the past focused on the acinar cell plasticity and on how the dedifferentiated acinar cells become duct-like (13), the inherent differences between the two cell populations that may underly a different propensity to tumor formation remained unclear. Therefore, we profiled, for the first time to our knowledge, the transcriptome of human dedifferentiated acinar cells versus their native duct cell counterpart. This comparative transcriptomic analysis provided

several new insights, including the fact that both cell populations were enriched in 'Pathways of cancer' although the related genes differed in both fractions. We identified MECOM, a transcription factor known to be involved in (pancreatic) cancer, as the most uniquely expressed gene in the dedifferentiated acinar cells.

MECOM is known to regulate many aspects of tumorigenesis including differentiation, proliferation and apoptosis (17-19, 40). It is a regulator of stomach-specific genes, some of which become upregulated in dedifferentiated acinar cells (23). Previously, a role for MECOM in pancreas cancer was proposed (20, 21, 37). Here, we focused on its role in acinar cell dedifferentiation. We uncovered that MECOM is uniquely expressed in dedifferentiated mouse and human acinar cells and absent from native duct cells, both in cell cultures and in tissue samples. Notably, MECOM expression levels appeared even higher in embryonic mouse pancreas, specifically in the pro-acinar tip cells again suggesting a relation to an immature acinar cell phenotype.

Interestingly, SOX9 is a known regulator of acinar cell dedifferentiation and a driver of pancreatic tumor formation (21, 48). Here, SOX9 expression correlated with that of MECOM. An interplay of MECOM and SOX9 has been described in other tissues (12, 13, 44) and we confirmed that SOX9 transactivates the *Mecom* enhancer in an acinar cell context. Still, it requires further investigation why SOX9 does not transactivate MECOM expression in duct cells where SOX9 expression is the highest.

We observed a clear phenotype when culturing MECOM deficient acinar cells (266-6 cells and primary mouse and human acinar cells), i.e. impaired formation of acinar domes or cell clusters, suggesting impaired cell adhesion and higher rates of apoptosis. We showed that MECOM depletion reduced the cell-cell interactions through *Itga2* and its ligands such as *Col4a2*. In our MECOM KO cells, the expression of several integrins (*Itga2, Itga4, Itga5 and Itga9*) was decreased. Importantly,

345 available ChIP-Seq data of MECOM in human ovarian carcinoma cells also showed
346 direct binding to the promotor regions of *Col4a2* and *Itga2* (43). We confirmed this in
347 MECOM KO cells, where reduced activity of the ERK signaling pathway could be
348 directly linked to reduced acinar cell dedifferentiation, a process for which this signaling
349 pathway is critical (12, 44). In a caerulein-induced acute pancreatitis model in MECOM-
350 deficient mice, we again make similar observations and demonstrated a prolonged
351 immune cell infiltration, similar as reported recently (37).
352 We propose that normal acinar cells have two options when they are subjected to
353 stress, either to subside in an “incognito” reversible dedifferentiated state, or to die.
354 MECOM seems indispensable for the former option. Ye et al., who, like us did not
355 provide formal proof by lineage tracing, claimed that MECOM-deficient acinar cells
356 transdifferentiate more extensively during pancreatitis (37). We suggest that MECOM-
357 deficient acinar cells undergo apoptosis and therefore cannot contribute any longer to
358 the CK19+ transdifferentiated cell pool. This is supported by our observations
359 increased inter-acinar spaces filled with fluid (edema) in the acute pancreatitis model.
360 Such phenotype has also been reported in EGF knockout mice (49). We also did not
361 detect any increase in collagen deposition around the recovering acini, which clearly
362 differs from acinar to ductal transdifferentiation that is accompanied by typical collagen
363 deposition (50), further supporting our conclusion.
364 Altogether, these results show that dedifferentiated acinar cells have a clearly distinct
365 gene expression profile compared to native duct cells. Under stress, MECOM
366 expression is turned on, downstream of SOX9, where it prevents acinar cell death and
367 allowing cellular dedifferentiation.
368
369

Acknowledgements

Biospecimens and clinical data were provided by the Australian Pancreatic Cancer Genome Initiative (APGI, www.pancreaticcancer.net.au), which is supported by an Avner Pancreatic Cancer Foundation Grant (www.avnersfoundation.org.au).

This work was supported by the Research Foundation Flanders (FWO) (Odysseus project and FWO research project to IR (FWOODYS12 and FWOAL931)). We thank Gunter Leuckx, Emmy De Blay, Veerle Laurysens, Geert Stangé, the laboratory of Liver Cell Biology Research Group at Vrije Universiteit Brussel and Flemish Institute of Biotechnology for expert technical assistance. We thank Patrick Jacquemin for providing the ElaCreERT mice, and Susumu Goyama and Mineo Kurokawa for providing the Evi-1 floxed mice.

Conflict of interest

The authors declare no competing financial interests

References

1. Rahib L, Smith BD, Aizenberg R, Rosenzweig AB, Fleshman JM, Matrisian LM. Projecting cancer incidence and deaths to 2030: the unexpected burden of thyroid, liver, and pancreas cancers in the United States. Cancer Res. 2014;74(11):2913-21.

2. Krah NM, De La OJ, Swift GH, Hoang CQ, Willet SG, Chen Pan F, et al. The acinar differentiation determinant PTF1A inhibits initiation of pancreatic ductal adenocarcinoma. Elife. 2015;4.

3. Direnzo D, Hess DA, Damsz B, Hallett JE, Marshall B, Goswami C, et al. Induced Mist1 expression promotes remodeling of mouse pancreatic acinar cells. Gastroenterology. 2012;143(2):469-80.

4. von Figura G, Morris JPt, Wright CV, Hebrok M. Nr5a2 maintains acinar cell differentiation and constrains oncogenic Kras-mediated pancreatic neoplastic initiation. Gut. 2014;63(4):656-64.

5. Kopp JL, von Figura G, Mayes E, Liu FF, Dubois CL, Morris JPt, et al. Identification of Sox9-dependent acinar-to-ductal reprogramming as the principal mechanism for initiation of pancreatic ductal adenocarcinoma. Cancer Cell. 2012;22(6):737-50.

6. De La OJ, Emerson LL, Goodman JL, Froebe SC, Illum BE, Curtis AB, et al. Notch and Kras reprogram pancreatic acinar cells to ductal intraepithelial neoplasia. Proc Natl Acad Sci U S A. 2008;105(48):18907-12.

7. Habbe N, Shi G, Meguid RA, Fendrich V, Esni F, Chen H, et al. Spontaneous induction of murine pancreatic intraepithelial neoplasia (mPanIN) by acinar cell targeting of oncogenic Kras in adult mice. Proc Natl Acad Sci U S A. 2008;105(48):18913-8.

8. Tuveson DA, Zhu L, Gopinathan A, Willis NA, Kachatrian L, Grochow R, et al. Mist1-KrasG12D knock-in mice develop mixed differentiation metastatic exocrine pancreatic carcinoma and hepatocellular carcinoma. Cancer Res. 2006;66(1):242-7.

9. Grippo PJ, Nowlin PS, Demeure MJ, Longnecker DS, Sandgren EP. Preinvasive pancreatic neoplasia of ductal phenotype induced by acinar cell targeting of mutant Kras in transgenic mice. Cancer Res. 2003;63(9):2016-9.

10. Guerra C, Schuhmacher AJ, Canamero M, Grippo PJ, Verdaguer L, Perez-Gallego L, et al. Chronic pancreatitis is essential for induction of pancreatic ductal adenocarcinoma by K-Ras oncogenes in adult mice. Cancer Cell. 2007;11(3):291-302.

11. Baldan J, Houbracken I, Rooman I, Bouwens L. Adult human pancreatic acinar cells dedifferentiate into an embryonic progenitor-like state in 3D suspension culture. Sci Rep. 2019;9(1):4040.

12. Houbracken I, de Waele E, Lardon J, Ling Z, Heimberg H, Rooman I, et al. Lineage tracing evidence for transdifferentiation of acinar to duct cells and plasticity of human pancreas. Gastroenterology. 2011;141(2):731-41, 41 e1-4.

13. Pinho AV, Rooman I, Reichert M, De Medts N, Bouwens L, Rustgi AK, et al. Adult pancreatic acinar cells dedifferentiate to an embryonic progenitor phenotype with concomitant activation of a senescence programme that is present in chronic pancreatitis. Gut. 2011;60(7):958-66.

14. Roy N, Malik S, Villanueva KE, Urano A, Lu X, Von Figura G, et al. Brg1 promotes both tumor-suppressive and oncogenic activities at distinct stages of pancreatic cancer formation. Genes Dev. 2015;29(6):658-71.

15. Lee AYL, Dubois CL, Sarai K, Zarei S, Schaeffer DF, Sander M, et al. Cell of origin affects tumor development and phenotype in pancreatic ductal adenocarcinoma. Gut. 2018.

16. Pinho AV, Chantrill L, Rooman I. Chronic pancreatitis: a path to pancreatic cancer. Cancer Lett. 2014;345(2):203-9.

17. Konantz M, Andre MC, Ebinger M, Grauer M, Wang H, Grzywna S, et al. EVI-1 modulates leukemogenic potential and apoptosis sensitivity in human acute lymphoblastic leukemia. Leukemia. 2013;27(1):56-65.

18. Rommer A, Steinmetz B, Herbst F, Hackl H, Heffeter P, Heilos D, et al. EVI1 inhibits apoptosis induced by antileukemic drugs via upregulation of CDKN1A/p21/WAF in human myeloid cells. PLoS One. 2013;8(2):e56308.

19. Glass C, Wuertzer C, Cui X, Bi Y, Davuluri R, Xiao YY, et al. Global Identification of EVI1 Target Genes in Acute Myeloid Leukemia. PLoS One. 2013;8(6):e67134.

20. Tanaka M, Ishikawa S, Ushiku T, Morikawa T, Isagawa T, Yamagishi M, et al. EVI1 modulates oncogenic role of GPC1 in pancreatic carcinogenesis. Oncotarget. 2017;8(59):99552-66.

21. Tanaka M, Suzuki HI, Shibahara J, Kunita A, Isagawa T, Yoshimi A, et al. EVI1 oncogene promotes KRAS pathway through suppression of microRNA-96 in pancreatic carcinogenesis. Oncogene. 2014;33(19):2454-63.

22. Desai BM, Oliver-Krasinski J, De Leon DD, Farzad C, Hong N, Leach SD, et al. Preexisting pancreatic acinar cells contribute to acinar cell, but not islet beta cell, regeneration. J Clin Invest. 2007;117(4):971-7.

23. Grimont A, Pinho AV, Cowley MJ, Augereau C, Mawson A, Giry-Laterriere M, et al. SOX9 regulates ERBB signalling in pancreatic cancer development. Gut. 2015;64(11):1790-9.

24. Goyama S, Yamamoto G, Shimabe M, Sato T, Ichikawa M, Ogawa S, et al. Evi-1 is a critical regulator for hematopoietic stem cells and transformed leukemic cells. Cell Stem Cell. 2008;3(2):207-20.

25. MacDonald RJ, Swift GH, Real FX. Transcriptional control of acinar development and homeostasis. Prog Mol Biol Transl Sci. 2010;97:1-40.

26. Baer R, Cintas C, Dufresne M, Cassant-Sourdy S, Schonhuber N, Planque L, et al. Pancreatic cell plasticity and cancer initiation induced by oncogenic Kras is completely dependent on wild-type PI 3-kinase p110alpha. Genes Dev. 2014;28(23):2621-35.

466 27. Elghazi L, Weiss AJ, Barker DJ, Callaghan J, Staloch L, Sandgren EP, et al.
467 Regulation of pancreas plasticity and malignant transformation by Akt signaling.
468 Gastroenterology. 2009;136(3):1091-103.
469 28. Wu CY, Carpenter ES, Takeuchi KK, Halbrook CJ, Peverley LV, Bien H, et al.
470 PI3K regulation of RAC1 is required for KRAS-induced pancreatic tumorigenesis in
471 mice. Gastroenterology. 2014;147(6):1405-16 e7.
472 29. Shi ZD, Lee K, Yang D, Amin S, Verma N, Li QV, et al. Genome Editing in
473 hPSCs Reveals GATA6 Haploinsufficiency and a Genetic Interaction with GATA4 in
474 Human Pancreatic Development. Cell Stem Cell. 2017;20(5):675-88 e6.
475 30. Tiyaboonchai A, Cardenas-Diaz FL, Ying L, Maguire JA, Sim X, Jobaliya C, et
476 al. GATA6 Plays an Important Role in the Induction of Human Definitive Endoderm,
477 Development of the Pancreas, and Functionality of Pancreatic beta Cells. Stem Cell
478 Reports. 2017;8(3):589-604.
479 31. Martinelli P, Carrillo-de Santa Pau E, Cox T, Sainz B, Jr., Dusetti N, Greenhalf
480 W, et al. GATA6 regulates EMT and tumor dissemination, and is a marker of response
481 to adjuvant chemotherapy in pancreatic cancer. Gut. 2017;66(9):1665-76.
482 32. Martinelli P, Madriles F, Canamero M, Pau EC, Pozo ND, Guerra C, et al. The
483 acinar regulator Gata6 suppresses KrasG12V-driven pancreatic tumorigenesis in
484 mice. Gut. 2016;65(3):476-86.
485 33. Longoni N, Kunderfranco P, Pellini S, Albino D, Mello-Grand M, Pinton S, et al.
486 Aberrant expression of the neuronal-specific protein DCDC2 promotes malignant
487 phenotypes and is associated with prostate cancer progression. Oncogene.
488 2013;32(18):2315-24, 24 e1-4.

489 34. Izutsu K, Kurokawa M, Imai Y, Maki K, Mitani K, Hirai H. The corepressor CtBP
490 interacts with Evi-1 to repress transforming growth factor beta signaling. Blood.
491 2001;97(9):2815-22.
492 35. Yuasa H, Oike Y, Iwama A, Nishikata I, Sugiyama D, Perkins A, et al. Oncogenic
493 transcription factor Evi1 regulates hematopoietic stem cell proliferation through GATA-
494 2 expression. EMBO J. 2005;24(11):1976-87.
495 36. Buonamici S, Chakraborty S, Senyuk V, Nucifora G. The role of EVI1 in normal
496 and leukemic cells. Blood Cells Mol Dis. 2003;31(2):206-12.
497 37. Ye J, Huang A, Wang H, Zhang AMY, Huang X, Lan Q, et al. PRDM3 attenuates
498 pancreatitis and pancreatic tumorigenesis by regulating inflammatory response. Cell
499 Death & Disease. 2020;11(3):187.
500 38. Schaffer AE, Freude KK, Nelson SB, Sander M. Nkx6 transcription factors and
501 Ptf1a function as antagonistic lineage determinants in multipotent pancreatic
502 progenitors. Dev Cell. 2010;18(6):1022-9.
503 39. Zhou Q, Law AC, Rajagopal J, Anderson WJ, Gray PA, Melton DA. A
504 multipotent progenitor domain guides pancreatic organogenesis. Dev Cell.
505 2007;13(1):103-14.
506 40. Garside VC, Cullum R, Alder O, Lu DY, Vander Werff R, Bilenky M, et al. SOX9
507 modulates the expression of key transcription factors required for heart valve
508 development. Development. 2015;142(24):4340-50.
509 41. Mateo F, Arenas EJ, Aguilar H, Serra-Musach J, de Garibay GR, Boni J, et al.
510 Stem cell-like transcriptional reprogramming mediates metastatic resistance to mTOR
511 inhibition. Oncogene. 2017;36(19):2737-49.

512 42. Jensen JN, Cameron E, Garay MV, Starkey TW, Gianani R, Jensen J.
513 Recapitulation of elements of embryonic development in adult mouse pancreatic
514 regeneration. Gastroenterology. 2005;128(3):728-41.
515 43. Bard-Chapeau EA, Jeyakani J, Kok CH, Muller J, Chua BQ, Gunaratne J, et al.
516 Ecotopic viral integration site 1 (EVI1) regulates multiple cellular processes important
517 for cancer and is a synergistic partner for FOS protein in invasive tumors. Proc Natl
518 Acad Sci U S A. 2012;109(6):2168-73.
519 44. Collins MA, Yan W, Sebolt-Leopold JS, Pasca di Magliano M. MAPK signaling
520 is required for dedifferentiation of acinar cells and development of pancreatic
521 intraepithelial neoplasia in mice. Gastroenterology. 2014;146(3):822-34 e7.
522 45. Means AL, Meszoely IM, Suzuki K, Miyamoto Y, Rustgi AK, Coffey RJ, Jr., et
523 al. Pancreatic epithelial plasticity mediated by acinar cell transdifferentiation and
524 generation of nestin-positive intermediates. Development. 2005;132(16):3767-76.
525 46. Stanger BZ, Stiles B, Lauwers GY, Bardeesy N, Mendoza M, Wang Y, et al.
526 Pten constrains centroacinar cell expansion and malignant transformation in the
527 pancreas. Cancer Cell. 2005;8(3):185-95.
528 47. Strobel O, Dor Y, Alsina J, Stirman A, Lauwers G, Trainor A, et al. In vivo lineage
529 tracing defines the role of acinar-to-ductal transdifferentiation in inflammatory ductal
530 metaplasia. Gastroenterology. 2007;133(6):1999-2009.
531 48. Tanaka M, Shibahara J, Ishikawa S, Ushiku T, Morikawa T, Shinozaki-Ushiku
532 A, et al. EVI1 expression is associated with aggressive behavior in intrahepatic
533 cholangiocarcinoma. Virchows Arch. 2019;474(1):39-46.
534 49. Ardito CM, Grüner BM, Takeuchi KK, Lubeseder-Martellato C, Teichmann N,
535 Mazur PK, et al. EGF receptor is required for KRAS-induced pancreatic tumorigenesis.
536 Cancer Cell. 2012;22(3):304-17.

50. Hamada S, Masamune A. Elucidating the link between collagen and pancreatic cancer: what's next? Expert Rev Gastroenterol Hepatol. 2018;12(4):315-7.

Figure Legends

Figure 1. RNAseq analysis identifies *MECOM* as uniquely expressed in dedifferentiated acinar cells. (a) Schematic overview of FACS-purification of human dedifferentiated acinar and duct cells, using acinar-specific UEA-1 lectin. (b) Immunofluorescent staining of FACS-purified dedifferentiated acinar (UEA-1+/CA19.9-) and duct (UEA-1-/CA19.9+) cells at day 4 with CD142 and CA19.9. DNA is labelled in blue. (c) Table of genes uniquely expressed in human dedifferentiated acinar cells (green) and duct cells. Selection limited to genes with BaseMean ≥ 1000, Log2FC ≥ 2 or ≤ -2 and P.adj ≤ 0,01. (d) KEGG pathways enriched (Adj. p-value < 0,01) in human dedifferentiated acinar cells (N=5).

Figure 2. MECOM is uniquely upregulated in dedifferentiated acinar cells and not in duct cells. (a) qPCR for MECOM on purified human dedifferentiated acinar (UEA-1+/CA19.9-) versus duct cells (UEA-1-/CA19.9+) after FACS isolation at day 4 of culture, compared to the mixed exocrine fraction at day of isolation (D0) (N=5; mean ± SD; ***p<0,005; One-way ANOVA with post-hoc Bonferroni correction). (b,c) RNA-ISH for MECOM on tissue from normal human pancreas (b) and human chronic pancreatitis (c) Scale = 50μM. Arrows indicate individual mRNA dots. (d,e) Immunofluorescent co-staining of human mixed exocrine fraction at day 4 of culture for MECOM and CD142 (d) and for MECOM and CK19 (e). Scale = 50μM. (f-i) RNA-ISH for *Mecom* and (j) *Mecom* expression level in normal mouse pancreas (f; dotted line indicates a normal duct, striped line indicates the outer edge of an islet), embryonic pancreas (g); E16.5

563 embryonic pancreas; dashed line indicates groups of tip cells) and in a mouse model
564 for acute (h) and chronic (i) pancreatitis. Scale = 50µM. (j) 5 individual microscopic
565 fields per replicate were quantified. (N=5; mean ± SD; *p<0,05; **p<0,01; One-way
566 ANOVA with post-hoc Bonferroni correction;).
567
568 **Figure 3. SOX9 regulates MECOM during acinar cell dedifferentiation.** (a) qPCR
569 for MECOM and SOX9 expression on human exocrine mixed fraction in culture over
570 time (day 1 to day 8). Each donor is indicated as a different colored line. (b) Immunoblot
571 for MECOM, SOX9 and actin as loading control on human exocrine mixed fraction in
572 culture over time. Representative blot from N=3 human donor samples. The different
573 isoforms of MECOM locus are indicated by arrows. (c) Generation of acinar-specific
574 (Elastase) Cre deletor mice with $Sox9^{ex5}$ flanked by loxP sites. Acinar-specific deletion
575 of SOX9 is performed in ElaCreERT;$Sox9^{f/f}$ versus control (ElaCreERT) littermates by
576 administering tamoxifen 3 times over a period of 5 days, followed by a two-week
577 washout. Acute pancreatitis is induced by administering caerulein by 7 hourly injections
578 for 3 days over a period of 5 days. Mice are sacrificed at day 4 after caerulein
579 administration. Immunohistochemical staining for SOX9 and RNA in situ hybridization
580 of *Mecom* mRNA expression in mouse pancreatic tissue after experimentally induced
581 acute pancreatitis in control (ElaCreERT) and acinar-specific Sox9 knockout
582 (ElaCreERT;$Sox9^{f/f}$) mice. Scale = 50µM. (N=3; **p<0.01; unpaired two-tailed t-test)
583 (d) Luciferase reporter assay in 266-6 cells, 48h after transfection. (mean ± SD; N=3;
584 ***p<0,001; one-way ANOVA with post-hoc Bonferroni correction)
585
586 **Figure 4. *Mecom* retains cell adhesion and survival in 266-6 cells.** (a) RNA in situ
587 hybridization (RISH) on control (NT-gRNA) and Mecom KO (gRNA3) 266-6 cells. Scale

588 = 200µM. (N=3; **p<0,01; unpaired two-tailed t-test). (b) Phase contrast images of
589 control (NT-gRNA) and Mecom KO (gRNA3) 266-6 cells. Scale = 200µM. (c) Absolute
590 number of cells at 96h after seeding 50.000 cells (mean ± SD; N=3; **p<0,01; unpaired
591 two-tailed t-test) (d) Cell viability measured relative to background levels of the culture
592 medium by CellTiter Glo assay (mean ± SD; N=3; ***p<0,001; unpaired two-tailed t-
593 test) (e) Immunofluorescent staining and quantification of cleaved caspase 3+ cells.
594 (N=3; **p<0,01; unpaired two-tailed t-test) (f) KEGG pathway analysis on differential
595 gene expression profiles after RNAseq analysis of MECOM wildtype versus MECOM
596 KO cells (N=3) (g) Venn diagrams showing genes overlapping between differentially
597 expressed genes in MECOM KO 266-6 cells and publicly available ChIP-seq dataset
598 from Bard-Chapeau et al. (43) (h) Schematic representation of our hypothesis. (i)
599 Collagen IV immunofluorescent staining on 266-6 NTgRNA and gRNA3-transduced
600 cultured cells. (j) Immunoblot for phospho-ERK and total ERK and quantifications of
601 pERK relative to total protein stain. (mean ± SD; N=3; *p<0,05; Unpaired two-tailed t-
602 test)
603
604 **Figure 5. *Mecom* retains cell adhesion and survival in cultured acinar cells.** (a)
605 Acinar cell-specific deletion of MECOM is performed by administering tamoxifen 3
606 times over a period of 5 days both subcutaneously and by gavage, followed by a two-
607 week washout period. Acute pancreatitis is induced by administering caerulein by 7
608 hourly injections for 3 days over a period of 5 days. Mice are sacrificed at day 4 after
609 caerulein treatment. (b,e) Phase contrast images and quantification of mean cluster
610 surface of ElaCreERT and ElaCreERT;*Mecom*$^{f/f}$ isolated acinar cells immediately after
611 isolation (D0) and at day 4 of culture (D4). Scale = 100µM. (c,f) Cleaved caspase 3
612 staining and quantification on ElaCreERT and ElaCreERT;*Mecom*$^{f/f}$ acinar cells at day

4 of culture. Scale = 25µM. *(*d,g) CK19 staining and quantification of ElaCreERT and ElaCreERT;*Mecom*$^{f/f}$ acinar cells at day 4 of culture. Scale = 25µM. (mean ± SD; N=6; *p<0,05; **p<0,01; two-way ANOVA with post-hoc Bonferroni correction.)

Figure 6. *Mecom* depletion in acinar cells *in vivo* causes pronounced cell death during recovery after caerulein-induced acute pancreatitis. (a) Acinar-specific deletion of MECOM is performed by administering tamoxifen 3 times over a period of 5 days, followed by a two-week washout period. Acute pancreatitis is induced by administering caerulein by 7 hourly injections for 3 days over a period of 5 days. Mice are sacrificed at day 4 and day 11 after caerulein administration. (b,f) H&E staining and quantification of acinar/non-acinar area ratio relative to day 4. (c,g) Cleaved caspase 3 immunohistochemical staining and quantification at day 4. (d,h) Collagen staining and quantification relative to day 4. Scale = 50µM. (e,i) CD3 staining and quantification relative to day 4 for ElaCreERT and ElaCreERT;*Mecom*$^{f/f}$ mice. Scale = 50µM. (mean ± SD, N=6, **p<0,01, ns = non-significant. two-way ANOVA with post-hoc Bonferroni correction)

Figure 1

a

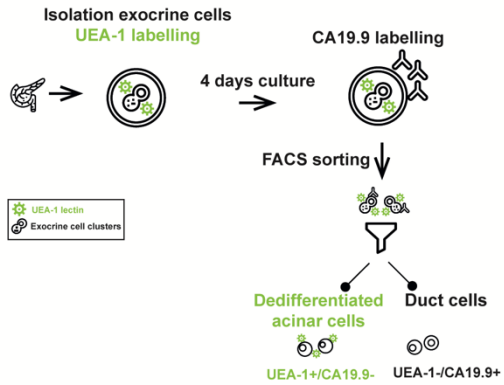

b

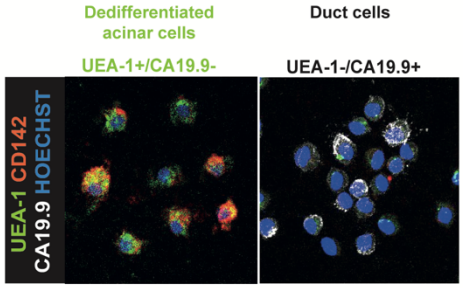

c

Dedifferentiated acinar cells (FC≤-2, adj.P≤0,01)	
Pathway	**Adj.P**
Protein digestion and absorption	1,185208E-11
Pancreatic secretion	1,267413E-10
Metabolic pathways	8,920072E-04
Pathways in cancer	2,494694E-03
Complement and coagulation cascades	2,704916E-03
Metabolism of xenobiotics by cytochrome P450	3,886956E-03
Fat digestion and absorption	3,953574E-03
Mineral absorption	3,953574E-03
PI3K-Akt signaling pathway	4,032070E-03
Drug metabolism - cytochrome P450	5,712517E-03
Steroid hormone biosynthesis	8,027015E-03
Glycine, serine and threonine metabolism	9,867525E-03

d

symbol	log2FoldChange	padj
DCD2	4,178944	7,066393E-126
MXRA5	-5,436366	1,103561E-129
GSTA2	-5,679022	2,094860E-159
IGFBP2	-5,777801	8,550959E-126
MGST1	-5,895840	1,446389E-147
MECOM	-6,091834	1,040978E-123
LGALS2	-4,859710	7,753555E-130

630

Figure 2

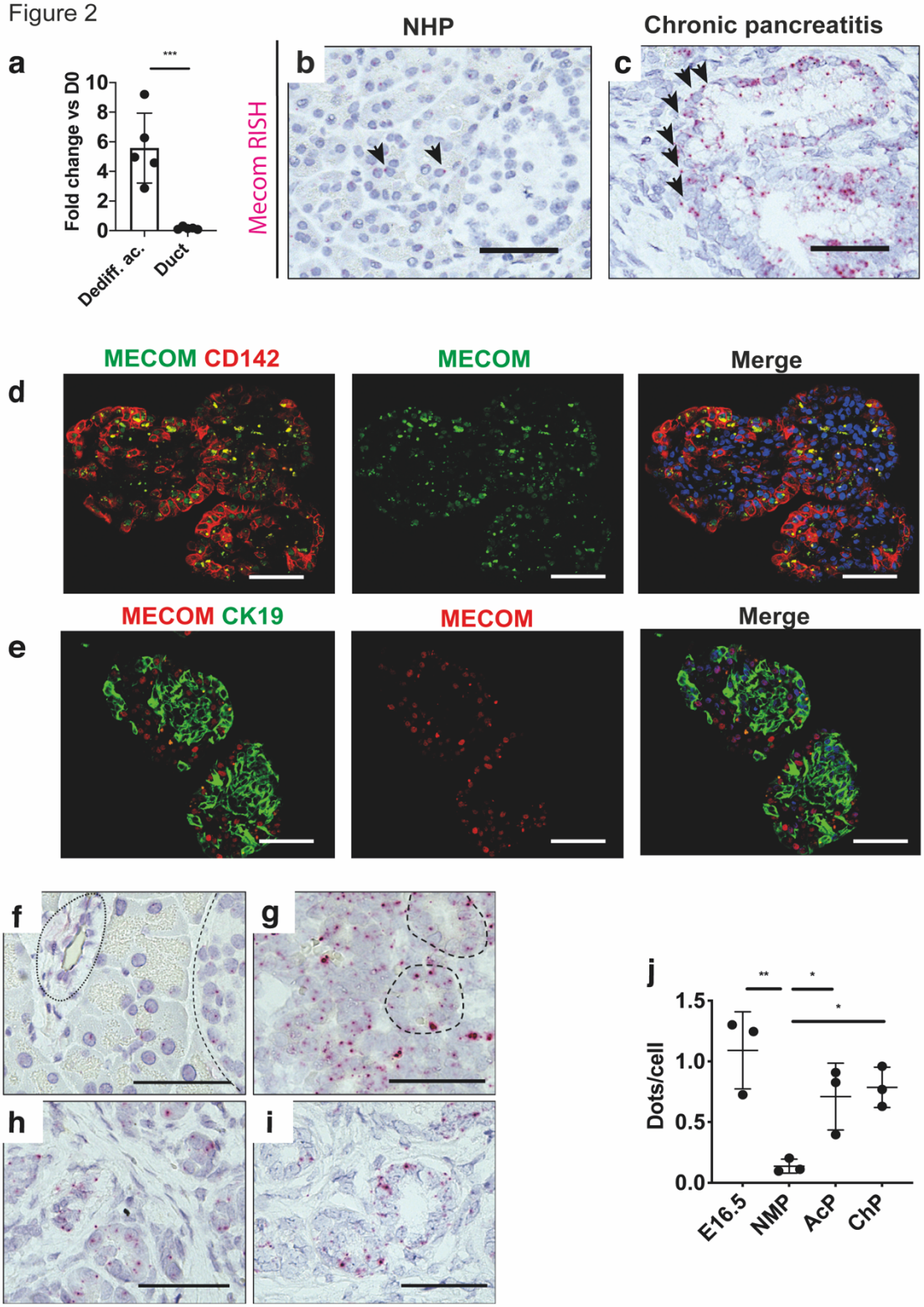

631

Figure 3

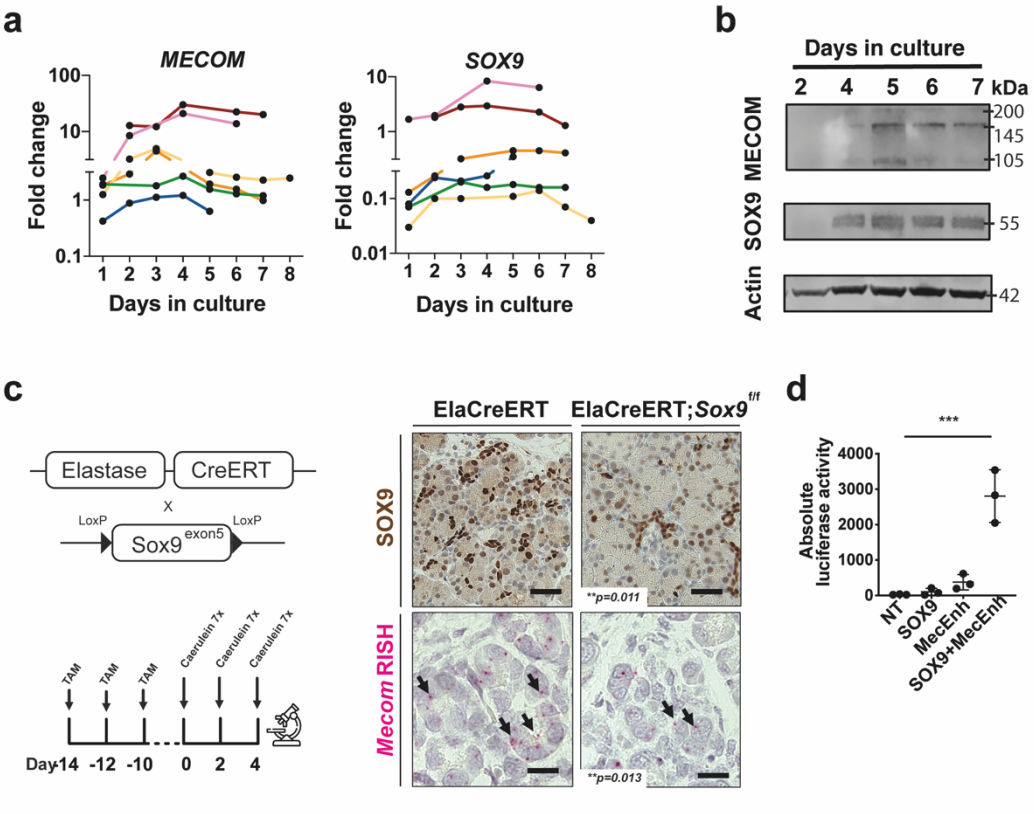

632

Figure 4

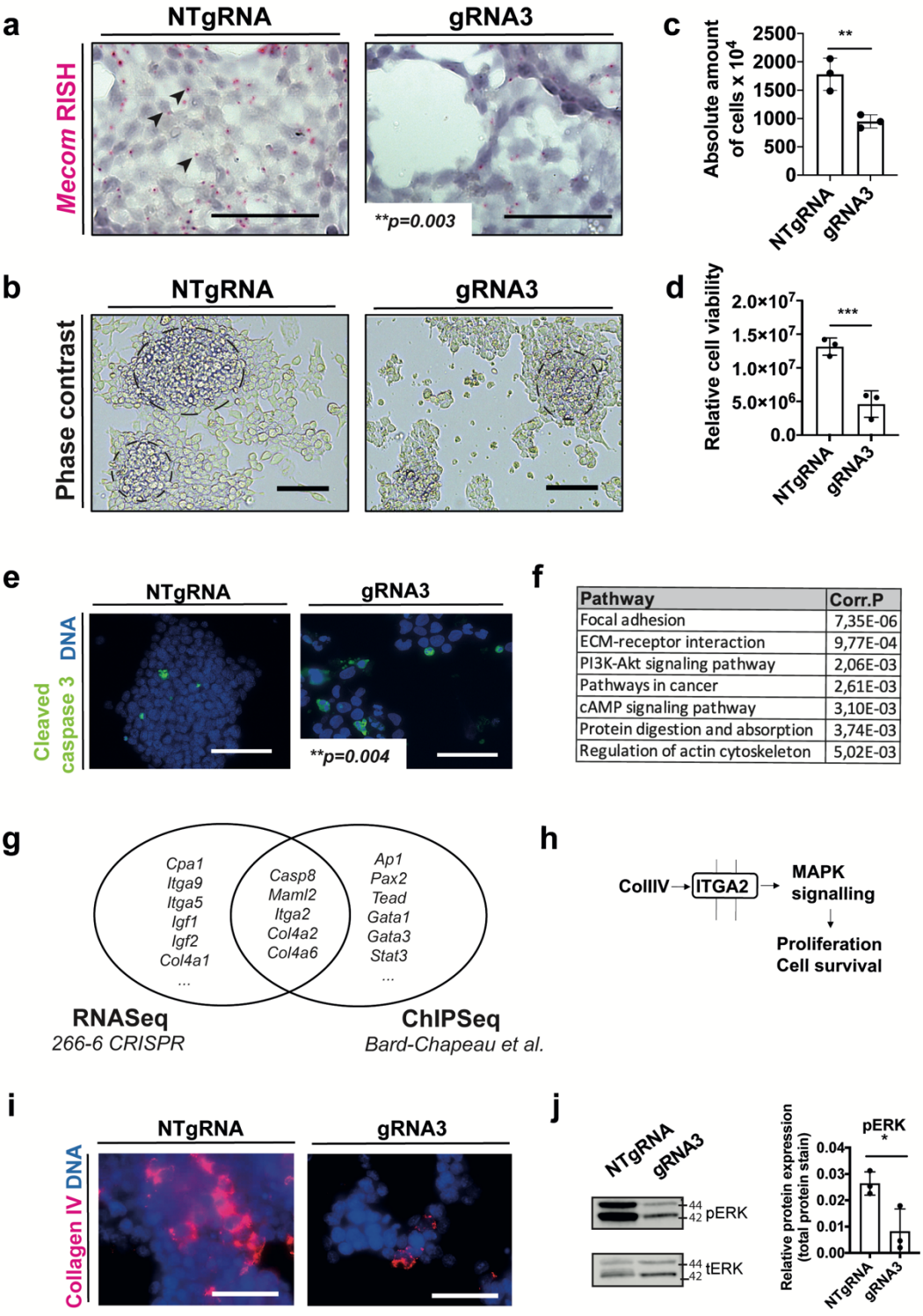

633

Figure 5

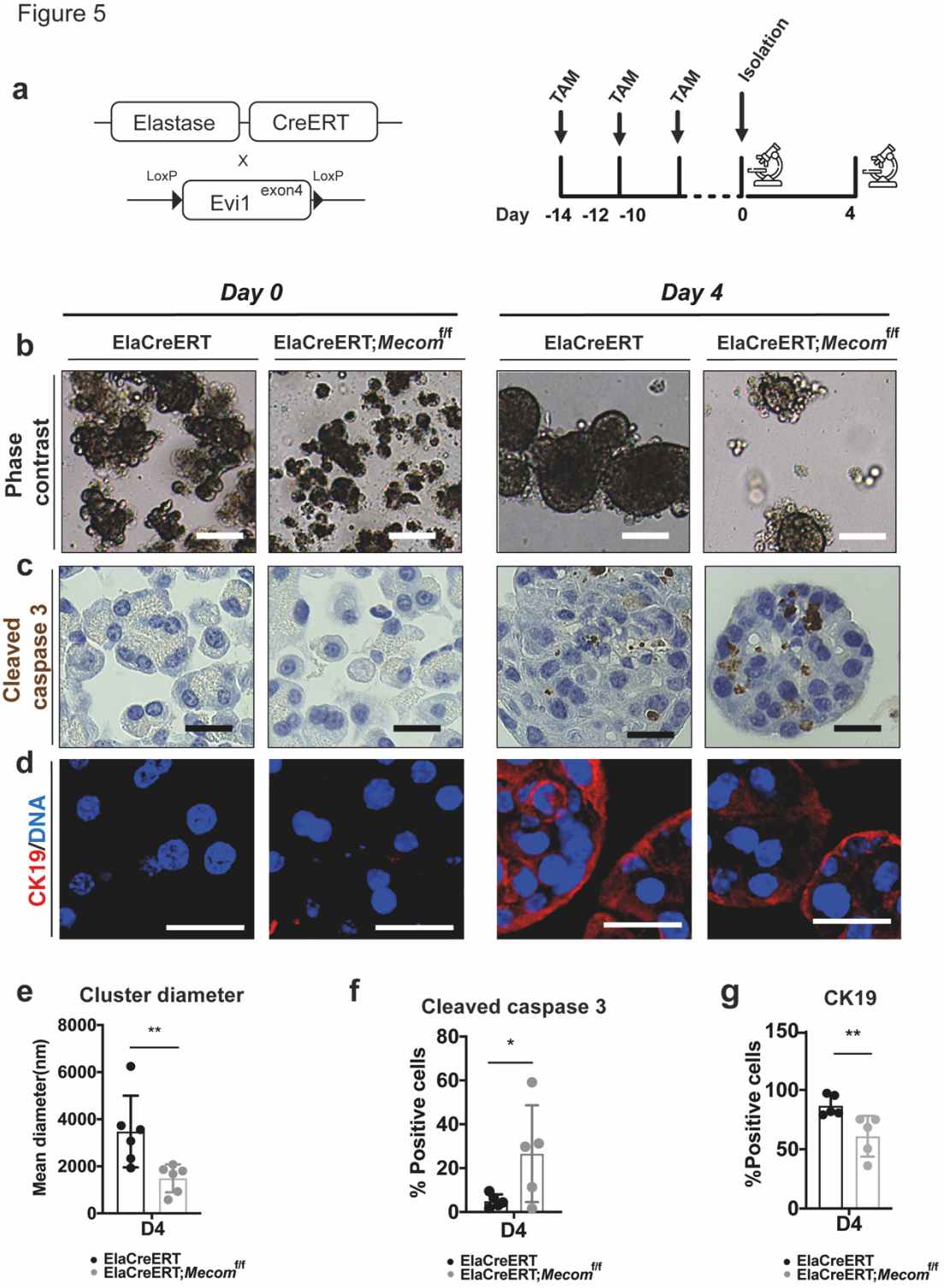

634

Figure 6

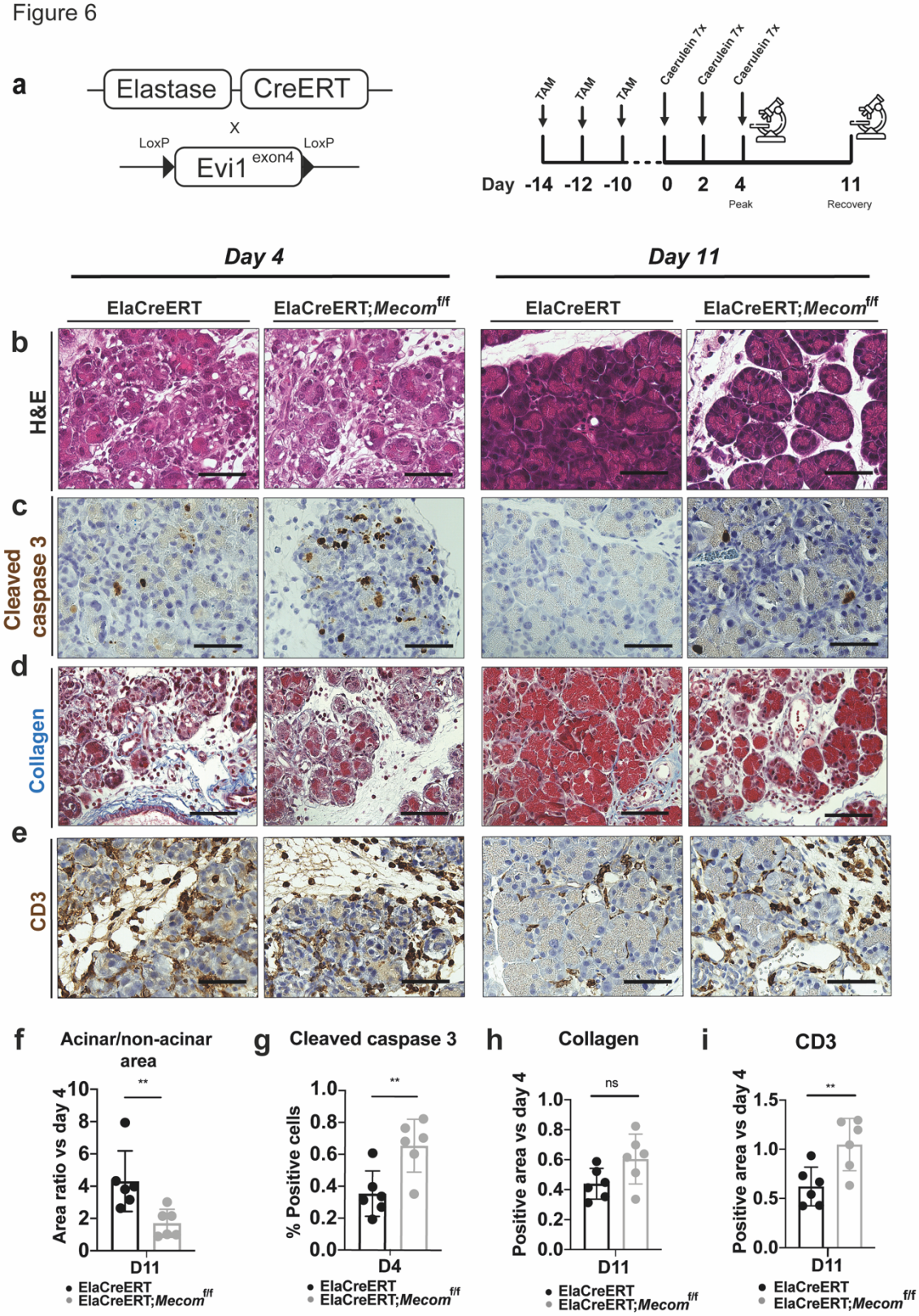

635